Miniature Electrodynamic Tethers to Enhance Picosatellite and Femtosatellite Capabilities

Iverson C. Bell, III
The University of Michigan
Ann Arbor, Michigan 48109, USA
(734) 763-6230
ICBell@umich.edu

Faculty Advisor: Brian E. Gilchrist
Electrical Engineering, The University of Michigan

Faculty Co-advisor: Sven G. Bilén
Electrical Engineering, The Pennsylvania State University

ABSTRACT

A new class of ultra-small satellites is emerging as a response to growing capabilities to integrate more functionality into an ever smaller volume. The satellites are categorized as picosatellites (100 g–1 kg) and femtosatellites (<100 g) and, due to their small size, they can be much less expensive to launch into orbit. In particular, it may be possible to deploy them in large numbers to enable missions requiring a distributed fleet of sensor spacecrafts (e.g., distributed aperture, simultaneous spatial sampling). However, without some degree of propulsion, these spacecraft would behave more as an uncontrolled *swarm rather than* a coordinated, controlled formation. Further, lifetime is limited for low-mass spacecraft with high area-to-mass ratios. This paper shows that a short, electrodynamic (ED) tether is capable of providing propellantless drag cancellation and even the ability to change orbit to picosatellites and femtosatellies in a range of altitudes in LEO. The ED tether can also be used as an antenna for communication to ground. Additionally, the paper describes the Miniature Tether Electrodynamics Experiment (MiTEE) CubeSat mission being developed to test the fundamental concept of short ED tethers for miniature spacecraft.

I. INTRODUCTION

New classes of sub-kilogram, "smartphone"-sized satellites are emerging as the next generation of miniaturized spacecraft. These potentially transformative satellite concepts have been motivated by the success of nanospacecraft (1–10 kg) and the terrestrial millimeter-scale, distributed wireless sensor concepts.[1,2] Growing interest in spacecraft with longest dimensions of only a few centimeters is the product of the increasing capability to integrate functionality and sophistication into even smaller volumes. Capability at this scale has been made possible by electronics miniaturization and reduced power consumption. Advances in integrated circuit (IC) and microelectromechanical systems (MEMS) technology make it possible to design satellites at the levels of hybrid integrated circuits or fully monolithic semiconductor integrated circuits. These satellites are categorized as picosatellites (100 g–1 kg), femtosatellites (<100 g), and here, more generally, as "ultra-small satellites" (≤1 kg).
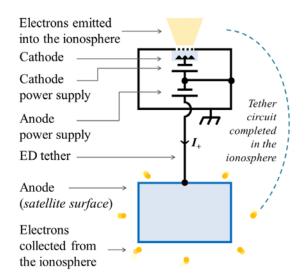
This trend implies that in the future, satellites near and below the 100-gram level could match or exceed the capabilities of modern nanosats. Owing to their small size and mass, pico- and femtosats can be significantly less expensive to develop, launch, and mass produce.[3] It is not expected, however, that individual pico- or femtosats will replace larger satellites in most missions; instead, it has been proposed that the goal of pico- and femtosatellites is to "do less with more," meaning that large numbers of simple but sufficiently capable satellites can *synergistically* perform a range of unique missions.[4] Coordinated *fleets* of these satellites, for example, could provide the ability to perform simultaneous, multi-point remote or *in situ* sensing and rapid re-measurement of a single location. These capabilities could fundamentally transform monitoring of natural disasters and space weather. References 3 and 4 offer additional potentially transformative mission concepts.
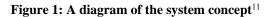
Natural environmental perturbations can de-orbit a satellite and modify a satellite formation over time. Perturbations like atmospheric drag and solar radiation

pressure have an especially strong influence on the dynamics of satellites at this size and mass scale.[5] Ultra-small satellites have inherently high area-to-mass ratios, so their orbital lifetimes in low Earth orbit (LEO) can be very short, ranging from a few months to just a few hours depending on altitude and solar condition.[6] Some form of propulsion would be necessary to increase mission lifetime and maintain or reconfigure a formation. Maneuverability is also essential for collision avoidance. Thus, appropriately-scaled propulsion systems play an important role in unlocking the potential of pico- and femtosatellites.

A variety of concepts have been proposed for ultra-small satellite propulsion.[7–9] However, while a satellite using consumable propellant can overcome atmospheric drag, the volume and mass of required propellant will increase unacceptably as the desired satellite lifetime increases. Adequate communication, attitude control, and energy generation also present significant challenges for satellites at this scale.

Previous trade studies have shown that a short (few meters long), semi-rigid electrodynamic (ED) tether has potential to provide propellantless propulsion for pico- and femtosats.[10] The concept is shown in Fig. 1. ED tethers can also be used for harvesting electrical energy from the orbit, allowing for propellantless, self-powered deorbiting.[11] Furthermore, this same tether could serve as an enhanced communication or scientific radio antenna aperture.[12] In this paper, previous studies are advanced, investigating how short tethers can enhance pico- and femtosat capabilities. Finally, the development of the Miniature Tether Electrodynamics Experiment (MiTEE) mission is described.

Figure 1: A diagram of the system concept[11]

I. TRADE STUDY BACKGROUND

A. Electrodynamic (ED) Tether Background

An electrodynamic tether (ED tether) is often thought of as a long conducting wire or cable, usually 100s of meters to kilometers in length, and is capable of propellantless altitude and inclination change. The ED tethers considered in this paper are a fundamentally new paradigm because they are much shorter, with total lengths less than 50 meters.

Tethers (conducting and non-conducting) experience a naturally occurring gravity-gradient torque that aligns the structure along the local vertical and a force on both ends that causes tension in the tether. The gravity-gradient force can be approximated by[13]

$$F_{\text{gravity–gradient}} \approx \frac{3m\mu L}{R_0^{\,3}}, \qquad (1)$$

where m is the total mass, R_0 is the distance from the spacecraft center of mass to the Earth's center, μ is the standard gravitational parameter of Earth, 3.986×10^{14} m$^3 \cdot$s^{-2}, and L is the length of the tether. If the gravity gradient torque dominates over other perturbation torques, the tether will naturally orient itself near the local vertical and liberate around it. This paper initially assumes a vertically aligned tether, although this assumption is evaluated later.

The orbital motion of an ED tether across Earth's magnetic field lines induces an electric field (i.e., *emf*) on the order of 0.1–0.25 V·m^{-1} for a low inclination orbit in LEO.[14] In a prograde orbit, the top end will be biased positive and the bottom end will be biased negative with respect to the surrounding ionosphere. The ionosphere is a plasma and can provide an electrical path to "complete the circuit" if both ends are equipped with a mechanism to exchange charge with the plasma. One approach is to collect electrons from the ionosphere using exposed conducting surfaces on the positive end (e.g., the anode) and emit electrons at the opposite end (e.g., the cathode).

The tether current interacts with the magnetic field to produce the Lorentz force, expressed as

$$\mathbf{F}_{\text{Lorentz}} = \int_0^L I_{\text{tether}} d\mathbf{L} \times \mathbf{B}, \qquad (2)$$

where I_{tether} is the tether current in segment dL and **B** is the magnetic field flux density vector. Final circuit closure occurs in the ambient plasma, satisfying Kirchhoff's Voltage Law. The *emf*-induced current can be harvested to supply energy to the spacecraft, but the resulting Lorentz force will oppose orbital motion and deboost the spacecraft. If a power supply provides a

voltage that exceeds the *emf*-induced bias, the thrust force can be used to maintain altitude or boost.

The Plasma Motion Generator (PMG) experiment demonstrated the ability to drive current along a tethered system in both directions using hollow cathode plasma contactors to electrically connect to the plasma. The Tethered Satellite System 1-Reflight (TSS-1R) tether demonstrated the ability to complete the circuit using a passive collection surface and an electron gun.[13]

B. System Concept Description

The miniaturized ED tether considered here is a short (several meters), insulated-but-conducting, semi-rigid tether connecting a pair of nearly identical pico- or femtosatellites that work together as a unit. Figure 1 shows an illustration of the basic concept. Each satellite has solar panels, a power supply, a cold cathode electron emitter, and is capable of collecting electrons on the surface. This way, the tether current could be reversed to change the direction of the force.

The dimensions of the satellites in this trade study are provided in Table 1. These dimensions have been influenced by a range of existing and proposed pico- and femtosat designs. The 200-g planar satellite is approximately the same size as PCBSat, a concept developed by the University of Surrey to be an element in a space-based wireless sensor network.[3] The 150-g cubic satellite takes its dimensions from the PocketQube. The PocketQube is an architecture that is increasing in popularity, with a single PocketQube unit (called "1P") equal to 1/8th of a standard 1U CubeSat in volume. TLogoQube, WREN, Eagle-1, and QubeScout-S1 are all PocketQube satellites that are currently on orbit.[15] The smaller 10-g ChipSat was inspired by Sprite. The Sprite femtosat concept was studied extensively and about 100 Sprites will be launched in the KickSat mission.[16]

Table 1: Satellite Dimensions

Description	Size	Drag Area
200-g planar satellite	10 cm × 10 cm × 2 cm	20 cm^2
150-g cubic satellite	5 cm × 5 cm × 5 cm	25 cm^2
10-g ChipSat	2.5 cm × 2.5 cm × 0.5 cm	1.25 cm^2

C. ED Tether Description

The miniaturized ED tether here is considered a "semi-rigid" structure. This is in contrast to much longer flexible tether systems with massive end-bodies, where the gravity-gradient would provide the tension necessary for deployment and stability in the presence of lateral forces (e.g., drag and solar radiation pressure). A material with a sufficient level of shape memory is desired for the tether to establish and hold its shape once deployed on orbit. However, the conducting strands should also be flexible enough to be spooled or coiled for storage until deployed on orbit. The ED tether prototype considered here has a Monel™ core to carry current and provide the needed level of rigidity. A thin layer of Teflon™ provides insulation. A highly conductive gold or silver coating on the Monel™ core has been considered for future designs to lower tether resistance.[10]

D. Trade Study Environment Assumptions

The altitudes considered are 400 km, 500 km, and 600 km in a circular, equatorial orbit. Following the same assumptions made in Ref. 17, the electron density was determined by averaging electron densities calculated at these altitudes at the equator using the International Reference Ionosphere-2007 (IRI-2007) model. This was done for January 1, 2000, which was a day with high solar activity in solar cycle 23 (F10.7D = 126). The neutral density was similarly taken from the Mass-Spectrometer-Incoherent-Scatter (MSIS-E-90) model. Atmosphere and ionosphere assumptions are summarized in Table 2. The assumed spacecraft velocity relative to the Earth's co-rotating atmosphere is 7.5 km·s^{-1}.[17]

Table 2: Ionospheric and Atmospheric Conditions[17]

Value	400-km Altitude	500-km Altitude	600-km Altitude
Electron Temp.	0.11 eV	0.14 eV	0.15 eV
Neutral Density	5×10^{-15} g·cm^{-3}	9×10^{-16} g·cm^{-3}	2×10^{-16} g·cm^{-3}
Electron Density	1×10^6 cm^{-3}	7×10^5 cm^{-3}	3×10^5 cm^{-3}
Debye Length	2 mm	3 mm	5 mm

II. Electron Emission

Electron emission needs to be well-characterized in order to neutralize the entire system and control the current flow in the tether. Field emitter array cathode (FEAC) technology offers the potential of an efficient means of emitting electrons into the ionosphere. Unlike hollow cathodes, FEACS do not require consumable expellant and no heater is required when compared to a thermionic electron emitter.

The satellites in this trade study assume the use of Spindt-style FEACs for electron emission.[18] The Spindt cathode has an array of sharp molybdenum cones, each cone on the scale of one micron in diameter and approximately the same in height. A bias is applied to a nearby grid or gate structure, which establishes an electric field (on the order of single $V \cdot nm^{-1}$) at the emitter tips. The large electric field at the tips allows electrons to quantum mechanically tunnel out of the tips and accelerate through the gate. The benefits of the field emitter array include its flat-panel scalability, meaning that it has a low profile and can fit very well into different faces of a small satellite. Storage on ground and robustness in the space environment remain important areas to investigate.

The Fowler–Nordheim law for electron field emission is[18]

$$I_{cathode} = A_{FN} V_{gate}^2 exp\left(b_{FN} \middle/ V_{gate}^2 \right), \qquad (3)$$

We assume the coefficients are $a_{FN} = 0.03$ $A \cdot V^{-2}$ and $b_{FN} = 487$ V, which are the coefficients determined from a 1-mm Spindt-style FEAC in laboratory conditions.[18]

III. Electron Collection

In our system concept, current will be collected by the positively biased exposed conducting surfaces of a pico- or femtosat. The surfaces will be biased well above the plasma potential to attract the current needed for propulsion. To increase the overall collection area, normally insulating surfaces like solar panels will be coated with a transparent conductor, e.g., Indium Tin Oxide (ITO).[19] However, estimating the actual collection current in the orbital environment is challenging. The likely shape and size of the pico- and femtosats, the relative drift of the plasma, and the ambient magnetic field all complicate predicting this current. Simplifying assumptions were made to estimate current in Ref. 12 and are summarized here.

A. The Spherical Sheath Model for Electron Collection

Current collection models provide a relationship between the anode voltage relative to the plasma potential and the collected current for geometries like spheres, infinite cylinders, and infinite plates. Pico- and femtosats, however, are sometimes planar and rectangular because components are mounted on printed circuit boards (PCBs) and/or silicon wafers. When a large bias is applied, it is assumed that the non-neutral sheath region between the immersed object's surface and the ambient plasma will balloon outwards, increasing the effective collection area, concealing the fine details of the electron collector's geometry, and allowing us to approximate it as spherical in shape. Current collection is estimated in this paper by assuming that the anode collects current like a sphere with an equivalent diameter equal to the satellite's longest edge.

B. Modeling the Electron Collector's Current–Voltage Characteristic

Reference 20 provides a strategy for extracting plasma parameters from the empirical current collection measurements in LEO. The expression[20]

$$I_{anode} = \frac{I_{thermal}}{2}\left(1 + \frac{q(V_{anode} - \Phi_p)}{kT_e} \right)^{\beta}, \qquad (4)$$

was fit to the Langmuir probe current–voltage (I–V) sweeps of the Wide Sweeping Langmuir Probe (WLP), a 5-cm-radius sphere, with varying values of the dimensionless parameter β. The thermal current $I_{thermal}$ is

$$I_{thermal} = A_{probe} n_e q \sqrt{\frac{kT_e}{2\pi m_e}}, \qquad (5)$$

and KT_e/q is the electron temperature in eV. We choose $\beta = 0.85$ for our model, which is close to the apparent average β value observed in the 2-hour time period shown in Ref. 20.

C. Experimental Assessment of Electron Collection Model

In order to evaluate the electron current collection assumptions mentioned above, a ground-based plasma experiment was conducted to capture key characteristics of the satellite-LEO interaction, like satellite geometry and high-speed plasma flow. The experimental facility was the cathode test facility (CTF) at University of Michigan's Plasmadynamics and Electric Propulsion Laboratory. The CTF is an aluminum cylindrical tank
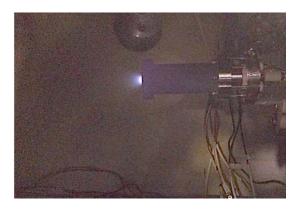

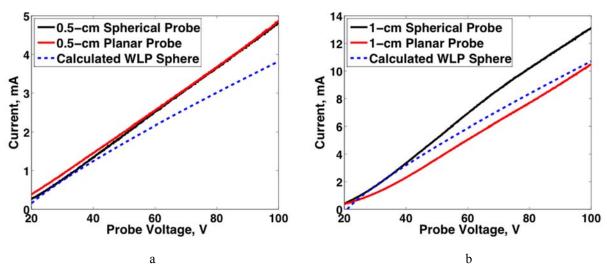**Figure 2: The LaB$_6$ hollow cathode and the plasma plume**

Figure 3a and b: Current–Voltage Characteristic of Spherical Probes (black) and Planar Probes (red) Compared to the Estimated Current Using Eq. 4 (blue) with β=0.85

that is approximately 60 cm in diameter and 2 m in axial length. A lanthanum hexaboride (LaB_6) hollow cathode, shown in Fig. 2, was constructed and used to simulate the relative velocity between the ionospheric plasma and the orbiting satellite. Xenon was the source gas in the experiment.

Initially, the test articles were positioned about 90 centimeters downstream from the hollow cathode and mounted on a motion stage so each measurement would take place in the same location. The probes are shown in Fig. 4 in the vacuum chamber. The test articles included two conducting plates that were 1 cm × 1 cm × 0.05 cm and 0.5 cm × 0.5 cm × 0.062 cm. The dimensions of the 1-cm and 0.5-cm test articles were selected to be *approximately* representative of a current collecting thin, flat, planar pico- or femtosat in the ionosphere after scaling with respect to Debye length (λ_D).

In the system modeling of current collection performance, it was assumed that the satellite would collect current like a sphere with an equivalent diameter equal to the satellite's longest edge. To assess this assumption experimentally, two spherical probes were tested that had diameters equal to the edge lengths of the two planar probes, i.e., a 1-cm diameter sphere and a 0.5-cm diameter sphere. A more complete description of the first iteration of the experiment is included in Ref. 12.

In the second iteration of the experiment, the probes were positioned 40 cm from the cathode to reduce the population of non-drifting charge exchange ions collected by the probes. This served to make the environment subtly more like LEO, where a satellite

interacts with a mesothermal plasma. Results presented here are from this second experiment.

Using the spherical Langmuir probes, the electron density was determined to be about 7×10^6 cm^3, the temperature about 1 eV, and the Debye length about 0.3 cm. In LEO, we expect a 0.1-eV to 0.2-eV plasma temperature with an electron density ranging from 10^4 cm^{-3} to 10^6 cm^{-3}.[21] The corresponding Debye length would be about 0.2–3.3 cm. In the experiment, the longest edge of the 0.5-cm planar probe would be *roughly* 1.5 times the Debye length and the longest edge of the 1-cm planar probe would be about 3 times the Debye length. Thus, the 1-cm planar probe could be more representative of a planar pico- or femtosat in a low density, large Debye length region of the ionosphere and
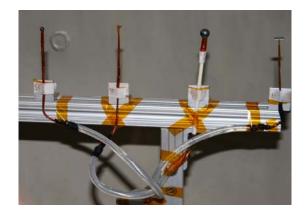

Figure 4: Probes Mounted in the Vacuum Chamber. *From left to right: 0.5-cm spherical probe, 0.5-cm planar probe, 1-cm spherical probe, and 0.5-cm planar probe*[11]

---

the 0.5-cm planar probe could be representative of a satellite in a slightly higher density, smaller Debye length region.

The current–voltage characteristics are shown in Figure 3. The system concept's anode will likely collect current in the electron saturation regime, so only voltages above the plasma potential are shown. The planar probes' current collection behavior is somewhat similar to that of the spherical probes, although there are some differences. The 0.5-cm planar probe current is about the same as the 0.5-cm spherical probe current. In this case, it is possible that the sheath masks the geometry of the small planar probe. However, the 1-cm planar probe collects slightly *less* current than the 1-cm spherical probe. The effect of the probe's shape is more apparent here, but additional experiments and simulations will be needed to better explain the behavior.

Additionally, the planar probe current collection characteristics can be compared to the current predicted by the WLP model. In the voltage range tested, the WLP model under predicts the collection current to the 0.5-cm planar probe by about 30% and over predicts the collection current to the 1-cm planar probe by 10–15%. The WLP-estimated current appears to level off with increasing potential more than the actual planar probe currents. Nevertheless, based on this limited data set, we believe that the WLP model provides a reasonable estimate for collection current. The results presented in this section build confidence in the model used to estimate current collection.

In future experiments, we would like to study the influence of a superimposed magnetic field on electron collection as well as use additional probe geometries.

IV. PROPULSION POWER ESTIMATE

Although the anode and cathode do not require consumable propellant to generate thrust, they require electrical power to conduct current through the tether. Pico- and femtosats generate very small amounts of power, and this translates into a limited amount of power available for propulsion. In previous iterations of this trade study, it has been shown that these picosats and femtosats are capable of generating sufficient power for ED tether drag make-up and boosting for a range of altitudes.[10] The same assumptions are made here with some minor differences to improve the accuracy of the estimate. A list of assumptions is provided in Table 3.

It is assumed that all 6 sides of the 200-g planar satellite and the 150-g cubic satellite have body-mounted solar cells, 3 of which face the sun at any given time. The 10-g ChipSat is much thinner, so it is assumed that it only has body-mounted solar cells on its 2 largest faces, one

facing the sun at a time. The factors believed to impact the power generated by the solar cells are the solar cell energy conversation efficiency (η_{sc}), the fraction of each face the solar cells cover (η_c), the total inherent degradation (η_{id}), lifetime degradation (η_{Ld}), efficiency due to ITO coating (η_{ITO}), and the "cosine loss" due to the solar angle (η_{sa}). The product of these efficiencies ($\eta_{cumulative}$) with the solar constant and the incident area give an estimate of generated power during daylight, or P_{sa}.

To boost throughout the entire orbit, the ultra-small satellites will needs to generate enough power on the dayside to meet all the power demands during the day (P_d) and eclipse (P_e). It is also important to account for the efficiency of distribution during daylight (X_d) and eclipse (X_e). The expression is given in by[13]

$$P_{sa} = \frac{\frac{P_e T_{ecl}}{X_e} + \frac{P_d T_d}{X_d}}{T_d},$$ (6)

where T_d and T_{ecl} are the length of the orbit in sunlight and eclipse, respectively. It is assumed that the power needed during day and night are approximately equal, or $P_d = P_e$, and that 70% of the overall power demand is available for ED tether propulsion, or $P_{EDT} = 0.7P_d$. As a result, the power available for ED tether propulsion is

$$P_{EDT} = 0.7\eta_{cumulative} \frac{T_d}{\frac{T_{ecl}}{X_e} + \frac{T_d}{X_d}} P_{inc},$$ (7)
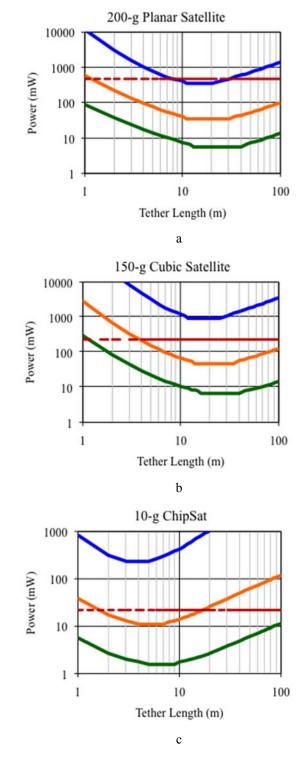
where P_{inc} is the combined incident solar and albedo power. As a result, the 200-g planar satellite, the 150-g cubic satellite, and the 10-g ChipSat can generate about 475 mW, 230 mW, and 22 mW, respectively. Our power generation estimates are consistent (on an order-of-magnitude basis) with the power generation estimates of other pico- and femtosat concepts.[3,4,7]
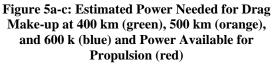
Table 3: Power Generation Estimate Assumptions

Solar constant, ϕ_{solar}		136.8 mW·cm^{-2}
Earth albedo, ϕ_{albedo}		41.0 mW·cm^{-2}
Solar cell energy conversion efficiency (GaAs)[13], η_{sc}		0.185
Coverage of each face, η_c		0.80
Total inherent degradation (combined effect of design, assembly, temperature, shadowing of cells)[13], η_{id}		0.72
Life degradation in 1 year[13], η_{Ld}		0.97
Efficiency due to ITO coating on solar cells[19], η_{ITO}		0.95
Average solar angle (45°), η_{sa}		0.70
Eq. 3 terms[13]	T_{ecl}	0.40
	T_d	0.60
	X_e	0.60
	X_d	0.80
Fraction of total generated power available for propulsion		0.70
Sun facing area, albedo facing area	200-g planar sat	140 cm^2 (sun), 100 cm^2 (albedo)
	150-g cubic sat	75 cm^2 (sun), 25 cm^2 (albedo)
	10-g ChipSat	~6 cm^2 (sun), 6 cm^2 (albedo)
Electrical power available for propulsion	200-g planar sat	475 mW
	150-g cubic sat	230 mW
	10-g ChipSat	22 mW

V. DRAG MAKE-UP CAPABILITIES WITH LIMITED POWER

The electrical power required to drive current through the tether is the sum of the power dissipated in the tether ($I_{tether}^2 R_t$), the power required to overcome *emf* ($I_{tether} V_{emf}$), and the power required by the anode ($I_{tether} V_{anode}$) and the cathode ($I_{tether} V_{gate}$). The impedance of the plasma is relatively small, so it is ignored. The power dissipated by the anode and cathode make up a majority of the electrical demand for the miniature tether application. The ohmic loss in the tether is not dominant because it scales with resistance and the square of current, both of which are relatively small. The *emf* is also small because the tethers are relatively short.

a

b

c

Figure 5a-c: Estimated Power Needed for Drag Make-up at 400 km (green), 500 km (orange), and 600 k (blue) and Power Available for Propulsion (red)

The drag make-up current can be estimated by setting the tether thrust in Eq. (2) equal to the atmospheric drag force (approximated as $I_{tether}=F_{drag}/LB$). The power required to generate the drag make-up current can be calculated by summing the power losses ($P_{tether}+P_{emf}+P_{anode}+P_{cathode}$). This value can then be compared against the power generated for ED tether thrust (P_{EDT}) to assess the feasibility of drag make-up.

Figures 5a–c compare the estimated power demand to the estimated power generated for propulsion. At each altitude considered, there is a tether length that minimizes the required drag make-up power. Very short ED tethers require relatively large current to overcome the atmospheric drag force on the ultra-small satellites. On the other hand, tether rigidity decreases with length, so a very long tether must have a larger radius to prevent severe bending or bowing. The current is minimized when these two effects are balanced. This motivates us to choose an 11-m long tether for the 200-g planar satellite, a 12-m tether for 150-g cubic satellite, and a 4-m tether for 10-g ChipSat. The tether lengths, radii, and currents are shown in Table 4. If drag make-up does not appear feasible because of the satellite's power generation limitations, the maximum available thrust power and the corresponding maximum achievable current and thrust are listed in italics in Table 4.
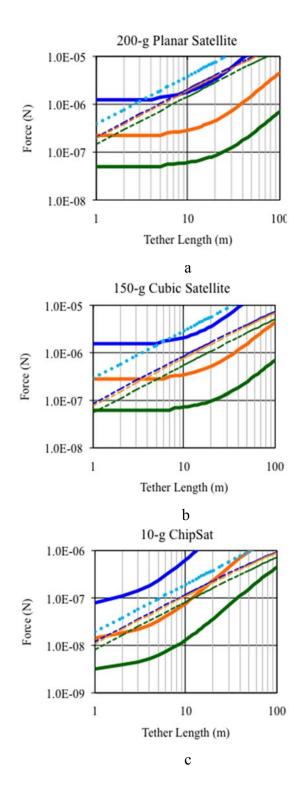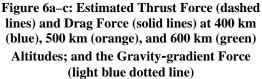
VI. FORCE ESTIMATE

The drag force and the gravity-gradient force are the dominant forces that impact the dynamics of tethered ultra-small satellites. Figures 6a–d show the thrust, atmospheric drag, and gravity-gradient force estimates for each satellite. Atmospheric drag is given by

$$F_{drag} = \tfrac{1}{2}\rho C_d A v^2 , \qquad (8)$$

where C_d is the coefficient of drag (assumed to be 2.2), ρ is the atmospheric neutral density, A is the cross-sectional ram area, and v is the satellite velocity. All three satellites show potential to generate a drag make-up force at the 500 km and 600 km altitudes. Only the 100-g planar satellite is able to produce thrust forces on par with drag at 400 km. The gravity-gradient force exceeds other forces at 400 km, 500 km, and 600 km except for the 10-g ChipSat at 400 km. This suggests that in other conditions the gravity gradient force will ensure a degree of stability. It may be possible for the 10-g ChipSat to use multiple tethers on several axes if attitude stability is not feasible.[22,23]

It will be important to study the relative strength of the drag and gravity gradient torques in order to understand the resulting tether attitude. If the center of mass and the center of pressure are vertically displaced, the

a

b

c

Figure 6a–c: Estimated Thrust Force (dashed lines) and Drag Force (solid lines) at 400 km (blue), 500 km (orange), and 600 km (green) Altitudes; and the Gravity-gradient Force (light blue dotted line)

aerodynamic drag torque will rotate the system. If the gravity-gradient torque is strong enough, however, it will counteract this rotation and restore the tether to an equilibrium along the local vertical.
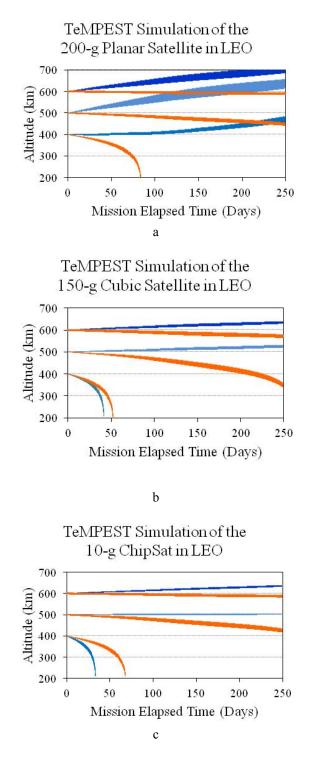
VII. PERFORMANCE SIMULATION

The software tool TeMPEST allows us to simulate an ED tether system in orbit. TeMPEST incorporates geomagnetic field models, ionospheric and atmospheric conditions, plasma contactor modeling, and precise orbital calculations to predict propulsion performance. We used TeMPEST to generate Fig. 7, which shows the altitude change of the pico- and femtosat with (blue) and without (orange) the ED tether propulsion at 400-km, 500-km, and 600-km starting altitudes. Rapid drag deboost can be seen without an ED tether, whereas actual boost capability is shown at 500 km and 600 km with a low-power, short ED tether. The 100-g satellite even shows potential to boost at 400 km.

Although the altitude curves in Fig. 7 appear to widen, this only represents increasing eccentricity of the satellite over time. This effect is particularly pronounced for ED tethers that are continuously boosting. The thrust force increases in regions of the ionosphere where the electron density is higher, and the uneven thrust in each orbit results in an increasing orbital eccentricity. However, ED tether boosting can be planned so the satellite orbit eccentricity degradation is minimized.[10]

VIII. OTHER BENEFITS: USING THE CONDUTING TETHER AS AN ANTENNA

Pico- and femtosatellites have small antenna apertures and low transmission power, but a conducting coating like gold or copper on the semi-rigid tether core (and underneath the insulation) would provide the potential for a long, directional, traveling wave antenna. The conducting layer would only need to be one or a few skin depths in thickness (on the order of micrometers, depending on frequency) to radiate with low resistive loss.

In previous studies, we modeled the radiation pattern of a satellite with dimensions similar to the 200-g planar satellite with a 10 m ED tether at 430 MHz using ANSYS® HFSS™ simulation software. The radiation pattern is shown in Figure 6. The antenna can be modeled as an off-centered dipole if a short wire, 10s of centimeters long (here 17 cm long), is attached to one of the tethered satellites. It was also found that the conducting 10 cm × 10 cm × 10 cm CubeSat structure is resonant at the UHF frequency, so the off centered dipole model with quarter wavelength pole and tether connected to the CubeSat have approximately the same radiation characteristics. The z-axis in Fig. 8 points in the nadir direction. With a small resonator in the tether line

a

b

c

Figure 7a–c: Simulation of a Single Satellite Starting at 400 km, 500 km, and 600 km Compared with Dual Satellites with an ED Tether

at the proper location, the antenna can also be adjusted for frequency and gain independent of its overall length.[10]
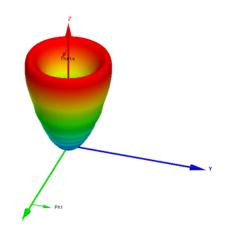

Figure 8: The 3D Radiation Pattern for a 10-meter-long Tether Radiating at 430 MHz
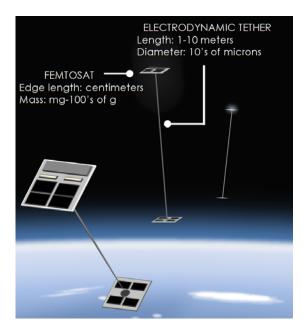

Figure 9: Concept of ED Tethers with Pairs of Femtosats as a Maneuverable, Coordinated Fleet

IX. POTENTIAL IMPACT

Using tethered pico- and femtosats with advanced, smart-phone like electronics and sensors, it may be possible to create carefully managed fleets of organized, spatially reconfigurable, capable sensor platforms. There are a variety of potential applications that lend themselves to this architecture.

Typical LEO satellite missions are single satellites that pass through a region every 90+ minutes. Also, they are limited to measuring scale sizes in the direction of travel of the satellite. A fleet of pico- or femtosats flying in an adaptable formation offers a significantly better potential to understand the phenomena that occur on small-, meso, and large-scales. Even simultaneous, distributed electron density and temperature measurements (e.g. from a Langmuir probe) could provide new understanding. Highly controlled fleets of pico- and femtosats could be carefully organized to explore our thermosphere and ionosphere (as well as other planets with an ionosphere and magnetic field, e.g. Jupiter). The tethered satellites themselves could act as double probes and collect electron and ion currents from the ambient environment on their exposed conducting surfaces. With this approach, the temporal (diurnal, seasonal, solar cycle) evolution of the ionosphere could be monitored in a fundamentally new way.

It may also be feasible to use a Global Positioning System (GPS) receiver on board one of the small satellites to make periodic total-electron-content (TEC) measurements or make measurements using ground based beacons over regions of interest (e.g., monitor amplitude and phase scintillation of GPS signals).[24] A better understanding of irregularities in the ionosphere could enhance GPS accuracy and terrestrial radio communication.[25]

Similarly, auroral zone measurements call for 3D placement of sensors (vertical and horizontal). The use of an on-board camera on each of the tethered satellites to provide a means of simple Earth surface monitoring is another example to be investigated.

Finally, if high levels of coordination can be achieved, a coordinated fleet of these satellites could be elements in a large, space-based, reconfigurable antenna array. The capabilities of such arrays are explored in Ref. 26. Tethered pico- or femtosatellites could also be connected to make large, sparse space structures.

X. MINIATURE TETHER ELECTRODYNAMICS EXPERIMENT (MITEE) SPACE MISSION DESCRIPTION

An in-orbit experiment is being planned by students at the University of Michigan to demonstrate the ultra-small satellite-ED tether concept in the space environment. The Miniature Tether Electrodynamics Experiment (MiTEE) mission is a technology demonstration mission that will utilize CubeSat capabilities to deploy a ChipSat-tether system and assess the key dynamics and electrodynamics essential to the system's successful operation. Starting as a 1U CubeSat,

Figure 10: MiTEE Mission Spacecraft Concept Showing the CubeSat Deploying the Picosat

a tethered picosatellite body of approximately 8 cm × 8 cm × 2 cm will be deployed from the CubeSat. The central questions motivating the mission include: (I) (Primary) Can the miniature tether provide stable, practical thrust for drag make-up and basic propulsion for "smart phone" sized ultra-small satellites? (II) (Secondary) Can the miniature tether and picosatellite system serve in other roles? This could include, among others, that the miniature tether could be the basis for a useful, enhanced antenna for communication with the ground.[12]

MiTEE is currently preparing for a high altitude balloon flight to evaluate the tether as an antenna and develop experience within the team for system integration. A microgravity flight presents the opportunity to test and study deployment in reduced gravity, so we are planning to complete a microgravity flight proposal in 2014. Additional risks associated with tether dynamics and generation of high voltage (50–200 V) for the anode and cathode will be analyzed with respective modeling.

XI. CONCLUSIONS

This study shows the potential of an ED tether to provide pico- and femtosats with propellantless maneuverability in a range of altitudes and also enhance communication. A summary of the system concept is shown in Table 4. If drag make-up is not feasible at a given altitude because the estimated power available for propulsion is insufficient, the maximum tether current and thrust force that can be provided are listed in italics.

There are several topics that will need to be investigated further to more completely show the feasibility of the concept. There are important practical questions that need to be addressed regarding tether storage and spooling, although some of these are being addressed in the MiTEE mission planning process. Also, although this study compares the magnitudes of the dominant forces on the spacecraft, the complex interaction of these forces will ultimately determine the spacecraft's ability to thrust and also influence its attitude. In addition, the electron field emission technology considered is extremely sensitive to surface contamination, so storage on ground and operation in LEO needs to be considered. Nevertheless, even with these questions, the miniature tethered satellite shows tremendous potential to enable a new paradigm in small satellite maneuverability.

Table 4: System Concept Summary

Parameter		200-g planar satellite	150-g cubic satellite	10-g ChipSat
Tether length		11 m	12 m	4 m
Tether radius		105 μm	110 μm	45 μm
Tether mass		2.7 g	3.4 g	150 mg
Available power		475 mW	230 mW	22 mW
Tether Current	400 km	5.9 mA	*2.8 mA*	*400 μA*
	500 km	0.9 mA	1 mA	230 μA
	600 km	0.2 mA	0.2 mA	5 μA
Thrust Force	400 km	2.3 μN	*1 μN*	*47 nN*
	500 km	2.1 μN	0.9 μN	44 nN
	600 km	1.6 μN	0.7 μN	33 nN
Gravity-gradient Force		4 μN	3.5 μN	77 nN

AKNOWLEDGEMENTS

REFERENCES

[1] Iyengar, S. S., and Brooks, R. R., *Distributed Sensor Networks, Second Edition: Image and Sensor Signal Processing*, CRC Press, 2012.

[2] Bouwmeester, J., and Guo, J., "Survey of worldwide pico- and nanosatellite missions, distributions and subsystem technology," *Acta Astronautica*, vol. 67, Oct. 2010, pp. 854–862.

[3] Barnhart, D. J., "Very Small Satellite Design for Space Sensor Networks," University of Surrey, 2008.

[4] Janson, S., and Barnhart, D., "The Next Little Thing: Femtosatellites," *AIAA/USU Conference on Small Satellites*, Aug. 2013.

[5] Atchison, J. A., and Peck, M. A., "Length Scaling in Spacecraft Dynamics," *Journal of Guidance, Control, and Dynamics*, vol. 34, 2011, pp. 231–246.

[6] Bell, I., "Electrodynamic Tethers for ChipSats and Nanospacecrafts," *11th Spacecraft Charging Technology Conference*, Albuquerque, NM: 2010.

[7] Atchison, J. A., and Peck, M. A., "A passive, sun-pointing, millimeter-scale solar sail," *Acta Astronautica*, vol. 67, Jul. 2010, pp. 108–121.

[8] Peck, M. A., Streetman, B., Saaj, C. M., and Lappas, V., "Spacecraft Formation Flying using Lorentz Forces," *Journal of the British Interplanetary Society*, vol. 60, 2007, pp. 263–267.

[9] Storck, W., Billett, O., Jambusaria, M., Sadhwani, A., Jammes, P., and Cutler, J., "A Survey of Micropropulsion for Small Satellites," *AIAA/USU Conference on Small Satellites*, Aug. 2006.

[10] Bell, I. C., McTernan, J. K., Gilchrist, B., and Bilen, S. G., "Investigating Miniature Electrodynamic Tethers and Interaction with the Low Earth Orbit Plasma," *AIAA SPACE 2013 Conference and Exposition*.

[11] Bilén, S. G., McTernan, J. K., Gilchrist, B. E., Bell, I. C., Voronka, N. R., and Hoyt, R. P., "Electrodynamic Tethers for Energy Harvesting and Propulsion on Space Platforms," *AIAA SPACE 2010 Conference & Exposition*, Anaheim, California: 2010.

[12] Bell, I., Gilchrist, B., Liaw, D., Singh, V., Hagen, K., Bilen, S., and McTernan, J., "Investigating the Potential of Miniaturized Electrodynamic Tethers to Enhance ChipSats," *The 33st International Electric Propulsion Conference*, Washington, DC: 2013.

[13] Wertz, J. R., Everett, D. F., and Puschell, J. J., *Space mission engineering: the new SMAD*, Hawthorne, CA: Microcosm Press : Sold and distributed worldwide by Microcosm Astronautics Books, 2011.

[14] Rasmussen, C. E., and Banks, P. M., "Theory of the electrodynamic tether," *Advances in Space Research*, vol. 8, Jan. 1988, pp. 203–211.

[15] "PocketQube," *Wikipedia, the free encyclopedia*, Apr. 2014.

[16] Manchester, Z., Peck, M., and Filo, A., "KickSat: A Crowd-Funded Mission to Demonstrate the World's Smallest Spacecraft," *AIAA/USU Conference on Small Satellites*, Aug. 2013.

[17] Bell, I., Gilchrist, B., Liaw, D., Singh, V., Hagen, K., Lu, C., Cutler, J., Bilén, S., and McTernan, J., "Investigating the Feasibility and Mission Enabling Potential of Miniaturized Electrodynamic Tethers for Femtosatellites and Other Ultra-small Satellites," *AIAA/USU Conference on Small Satellites*, Aug. 2013.

[18] Whaley, D. R., Duggal, R., Armstrong, C. M., Bellew, C. L., Holland, C. E., and Spindt, C. A., "100 W Operation of a Cold Cathode TWT," *IEEE Transactions on Electron Devices*, vol. 56, May 2009, pp. 896–905.

[19] McTernan, J. K., Brubaker, T. R., and Bilen, S. G., "Indium tin oxide coverings on solar panels for plasma-Spacecraft connection," *Photovoltaic Specialists Conference (PVSC), 2013 IEEE 39th*, 2013, pp. 2821–2826.

[20] Barjatya, A., Swenson, C. M., Thompson, D. C., and Jr, K. H. W., "Invited Article: Data analysis of the Floating Potential Measurement Unit aboard the International Space Station," *Review of Scientific Instruments*, vol. 80, Apr. 2009, p. 041301.

[21] Hastings, D., and Garrett, H. B., *Spacecraft-environment interactions*, Cambridge: Cambridge University Press, 2004.

[22] Voronka, N. R., Hoyt, R. P., Slostad, J., Gilchrist, B. E., and Fuhrhop, K., *Modular Spacecraft with Integrated Structural Electrodynamic Propulsion*, NASA Institute for Advanced Concepts, 2006.

[23] Weis, L., and Peck, M., "Attitude Control for Chip Satellites using Multiple Electrodynamic Tethers," *AIAA/AAS Astrodynamics Specialist Conference*, Minneapolis, Minnesota: American Institute of Aeronautics and Astronautics, 2012.

[24] Warnant, R., and Pottiaux, E., "The increase of the ionospheric activity as measured by GPS," *Earth, Planets and Space*, vol. 52, 2000, pp. 1055–1060.

[25] Wernik, A. W., Alfonsi, L., and Materassi, M., "Ionospheric irregularities, scintillation and its effect on systems," *Acta geophysica polonica*, vol. 52, 2004, pp. 237–249.

[26] Helvajian, H., and Janson, S. W., *Small satellites: past, present, and future*, El Segundo, Calif.; Reston, Va.: Aerospace Press ; American Institute of Aeronautics and Astronautics, 2008.